

## Some mineral physics constraints on the rheology and geothermal structure of Earth's lower mantle

DAISUKE YAMAZAKI\* AND SHUN-ICHIRO KARATO

### ABSTRACT

We explore the implications of recent mineral physics measurements of diffusion coefficients and melting temperatures of lower mantle materials on the rheological and geothermal structure of Earth's lower mantle. We show that  $\text{MgSiO}_3$  perovskite is significantly stronger than  $\text{MgO}$  periclase and therefore the rheology of the lower mantle depends strongly on the geometry of a weaker phase, periclase. We calculate viscosities of the lower mantle for two cases: (1) where periclase occurs as isolated grains and (2) where periclase occurs as continuous films, using mineral physics data and models of two-phase rheology. We find that the effective viscosity for the former is about  $\sim 10$ – $1000$  times higher than the latter. We therefore suggest that the rheology of the lower mantle is structure- and hence strain-dependent, leading to weakening at large strains due to the formation of continuous films of periclase. Overall depth variation of viscosity depends not only on the pressure dependence of creep but also on the geothermal gradient. Both  $\text{MgSiO}_3$  perovskite and periclase have relatively small activation energies ( $E^* = gRT_m$  with  $g = 10$ – $14$ , where  $R$  is the gas constant and  $T_m$  is melting temperature), and therefore the depth variation of viscosity is rather small, even for a nearly adiabatic temperature gradient. However, the geothermal gradients consistent with the geodynamical inference of nearly depth-independent viscosity are sensitive to the pressure dependence of viscosity which is only poorly understood. A superadiabatic gradient of up to  $\sim 0.6$  K/km is also consistent with mineral physics and geodynamical observations.

### INTRODUCTION

The lower mantle occupies  $\sim 65\%$  of Earth's mantle and therefore its dynamics delineates the thermal evolution and the dynamics of the whole Earth. However, until recently, experimental studies relevant to lower mantle rheology have been difficult and few mineral physics constraints had been obtained. As a result, most of the previous studies used either theoretical estimates of rheology using some empirical relations (e.g., Karato 1981a) or were based on the experimental results on some analog materials (e.g., Poirier et al. 1983; Karato and Li 1992; Li et al. 1996). However, the situation has changed during the last few years due to advances in high-pressure experimentation. For example, Yamazaki et al. (2000) measured the self-diffusion coefficients of silicon in  $\text{MgSiO}_3$  perovskite under shallow lower mantle conditions. The kinetics of grain growth in a lower mantle assembly (perovskite-periclase mixture) were investigated by Yamazaki et al. (1996). In addition, melting temperatures of lower mantle minerals have been determined experimentally (e.g., Zerr and Bohler 1993, 1994; see also Wang 1999). Furthermore, some progress has been made in modeling the rheology of a two-phase mixture. Handy (1994) and Takeda (1998), for example, proposed theoretical models for the deformation of a two-phase mixture. Such models underline the importance of the geometry of a weaker phase as well as its volume fraction.

Progress has simultaneously occurred in geophysical studies relevant to lower mantle rheology. Seismological observations strongly indicate a nearly isotropic lower mantle (e.g., Meade et al. 1995; Garnero and Lay 1997). This observation has been interpreted to suggest an importance of diffusional creep as a dominant deformation mechanism (Karato et al. 1995). Second, some new constraints have been obtained on the viscosity-depth relationship using the analysis of relative sea level change data as well as the analysis of geoid anomalies (e.g., Mitrovica and Forte 1997). These results show that the viscosities of the lower mantle are significantly higher than those of the upper mantle, but the depth variation in viscosity in the lower mantle is only modest (less than a factor of  $\sim 10$ ). The purpose of this paper is to combine these new mineral physics developments with geophysical observations to place some constraints on rheology and geothermal structure of Earth's lower mantle.

### DIFFUSION CREEP IN THE LOWER MANTLE MATERIALS

Plastic deformation of rocks occurs either by motion of dislocations (dislocation creep) or by the diffusive transport of individual atoms (diffusion creep) (e.g., Frost and Ashby 1982). Deformation by dislocation creep causes significant lattice preferred orientation, but diffusion creep does not (Karato 1988; Karato et al. 1995). Because lower mantle materials [ $(\text{Mg,Fe})\text{SiO}_3$  perovskite and  $(\text{Mg,Fe})\text{O}$  magnesiowüstite] have significant elastic anisotropy, deformation due to dislocation creep would result in significant seismic anisotropy. Recent

\* E-mail: yamaz002@tc.umn.edu

seismological observations show that a large part of the lower mantle is isotropic (Meade et al. 1995; Montagner and Kennett 1996; Garnero and Lay 1997), although significant anisotropy occurs in the D'' layer (Garnero and Lay 1997). Therefore, the lack of seismic anisotropy in most of the lower mantle suggests the importance of diffusion creep in lower mantle dynamics (Karato et al. 1995). Consequently, we consider only diffusion creep in this paper. We first calculate the viscosity of both components of the lower mantle, which are approximated by the end-members, MgSiO<sub>3</sub> perovskite and periclase. [The effects of other elements (Fe, Ca, Al, etc.) will be discussed below.] We then calculate the viscosity of the lower mantle by taking an appropriate average of viscosities of these two phases.

In the diffusion creep regime, the effective viscosity of a given mineral is related to the diffusion coefficient through

$$\frac{1}{\eta} = A \frac{\Omega}{RT} \frac{D_{\text{eff}}}{G^2} \quad (1)$$

where  $A$  is a constant ( $\sim 13.3$ ),  $\Omega$  is the molar volume,  $R$  is the gas constant,  $T$  is absolute temperature,  $D_{\text{eff}}$  is the effective diffusion coefficient, and  $G$  is grain size of the constituent materials (e.g., Frost and Ashby 1982). The effective diffusion coefficient in a compound is related to the diffusion coefficients of individual species as

$$D_{\text{eff}} = 1 / \sum_i \left( n_i / \tilde{D}^i \right) \quad (2)$$

where  $n_i$  is the stoichiometric coefficient of the  $i$ -th species and  $\tilde{D}^i$  is the diffusion coefficient of the  $i$ -th species (Stocker and Ashby 1973). In polycrystalline materials, mass transportation is controlled by the effective diffusion coefficient through the bulk of grains as well as along grain boundaries, viz.,

$$\tilde{D}^i = D_i^l + (\pi \delta / G) D_{\text{gb}}^i \quad (3)$$

where  $D_i^l$  and  $D_{\text{gb}}^i$  are the lattice and grain boundary diffusion coefficients of the  $i$ -th species, respectively, and  $\delta$  is the width of grain boundary (e.g., Frost and Ashby 1982).

Therefore, given both lattice and grain-boundary diffusion coefficients of all the atomic species in lower mantle minerals under lower mantle conditions, the effective viscosity of lower mantle minerals can in principle be calculated from the assumed grain-size and temperatures. Temperature is also an important parameter. In the present calculations, the temperature at 660 km is assumed to be 1873 K (Ito and Katsura 1989). Considering the uncertainties in the temperature profile, we use a range of geothermal gradients. It is also necessary to use a theoretical model to extrapolate laboratory data to the deep lower mantle.

Critical to these studies are (1) the diffusion coefficients and flow law parameters in diffusion creep in lower mantle minerals and (2) the pressure dependence of diffusion coefficients. The next section reviews these issues.

Diffusion creep in MgO has been studied extensively (e.g., Gordon 1985). We use these results and extrapolate them to higher pressures using theoretical models for pressure depen-

dence of diffusion. The experimental studies contain complexities caused by the presence of multiple diffusing species and diffusion paths. In MgO, diffusion along grain boundary is significantly enhanced for O but not for Mg, leading to  $[D_1^{\text{Mg}} + (\pi \delta / G) D_{\text{gb}}^{\text{Mg}}] < [D_1^{\text{O}} + (\pi \delta / G) D_{\text{gb}}^{\text{O}}]$ . Consequently, the rate of deformation is controlled by the lattice diffusion of Mg. Similarly, diffusion of Mg (or Fe) under dry conditions has been suggested to control diffusion creep in olivine (Karato et al. 1986).

Therefore, not only lattice diffusion coefficients but also grain-boundary diffusion coefficients are needed to estimate the viscosity resulting from diffusion creep. For many silicate minerals, the slowest diffusion species is Si (e.g., Jaoul et al. 1981, 1983). Moreover, theoretical calculations of diffusion coefficients in MgSiO<sub>3</sub> perovskite suggest that Si is the slowest diffusing species and O is the fastest through the bulk (Wall and Price 1989). Recent experimental study (Yamazaki et al. 2000) determined the lattice and grain-boundary diffusion coefficients of Si in MgSiO<sub>3</sub> perovskite under shallow lower mantle conditions. They showed that grain-boundary diffusion of Si is not very important in MgSiO<sub>3</sub> perovskite under most cases (Fig. 1). Therefore the lattice diffusion of silicon should control the rate of deformation due to diffusion creep in MgSiO<sub>3</sub> perovskite. Below, we will calculate the viscosity of MgSiO<sub>3</sub> perovskite by extrapolating the experimental data for silicon diffusion (Yamazaki et al. 2000) and the viscosity of MgO by extrapolating the experimental data of diffusion creep (Passmore et al. 1966).

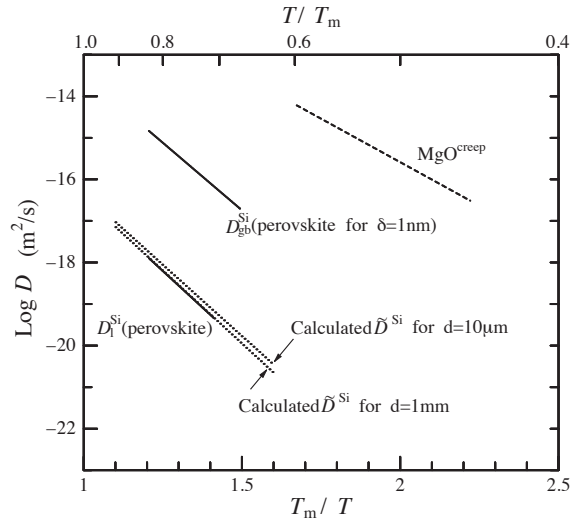


**FIGURE 1.** Silicon self-diffusion coefficients in MgSiO<sub>3</sub> perovskite and the calculated diffusion coefficient of MgO are plotted against normalized temperature ( $T/T_m$ ) based on Yamazaki et al. (2000) and Passmore et al. (1966). Solid lines represent the lattice and grain boundary diffusion coefficients in MgSiO<sub>3</sub> perovskite, assuming 1 nm width for the grain boundary. Dotted lines show the calculated diffusion coefficient at a grain size of 10  $\mu\text{m}$  and 1 mm. Dashed line shows the calculated effective diffusion coefficient in MgO from creep tests.

### PRESSURE DEPENDENCE OF DIFFUSION

Some extrapolations of the diffusion coefficients to high pressure are needed to determine the viscosity profile in the lower mantle, because the experimental data were obtained at 25 GPa for  $\text{MgSiO}_3$  perovskite and at room pressure for  $\text{MgO}$ . The dependence of diffusion coefficients on pressure is represented by the change of activation enthalpy  $H^*(P)$  as

$$D = D_0 \exp[-H^*(P)/RT] \quad (4)$$

where the pre-exponential factor  $D_0$  is a constant and  $P$  is pressure. It is impossible to evaluate the pressure dependence of  $H^*(P)$  experimentally because of the lack of experimental data. Therefore, we use two empirical models (homologous temperature scaling and an elastic strain energy model) to evaluate the pressure dependence of diffusion.

### Homologous temperature scaling

Many experimental data show a good correlation between activation enthalpy and melting temperature (e.g., Sherby et al. 1970; Weertman 1970; Sammis et al. 1980; Karato 1981b), viz.

$$H^*(P) = gRT_m(P) \quad (5)$$

where  $g$  is a non-dimensional constant and  $T_m(P)$  is the melting temperature at pressure  $P$ . In this case, Equation 4 is modified to

$$D(P, T) = D_0 \exp[-gT_m(P)/T] \quad (6)$$

where  $T/T_m$  is referred to as homologous temperature. For  $T_m(P)$ , we use the melting temperature of each phase, and estimate the viscosity of each phase separately. The effect of mixing two phases will be considered in the next section. There are large uncertainties in laboratory measurements of melting temperatures of lower mantle minerals. We use the results compiled by Wang (1999) for  $\text{MgSiO}_3$  perovskite (Fig. 2A) and the results by Zerr and Bohler (1994) for  $\text{MgO}$ .

Using the activation enthalpy for silicon diffusion (Fig. 1) and the melting temperature at 25 GPa, the constant  $g$  of  $\text{MgSiO}_3$  perovskite can be determined to be  $\sim 14$  (Eq. 5), whereas that of  $\text{MgO}$  is  $\sim 10$ . From these values, we estimated the activation enthalpy at higher pressure using the melting curve of  $\text{MgSiO}_3$  perovskite and  $\text{MgO}$  (Fig. 2B). Because both the constant  $g$  and the slope of the melting curve ( $dT_m/dP$ ) for  $\text{MgO}$  are smaller than those for  $\text{MgSiO}_3$  perovskite, the activation enthalpy of  $\text{MgO}$  at the bottom of the lower mantle is much smaller than that of  $\text{MgSiO}_3$  perovskite (Fig. 2B). When the first order derivative with respect to the pressure is taken, Equation 5 gives,

$$V^* = gR(dT_m/dP) \quad (7)$$

Using this equation, the activation volume at 25 GPa for homologous temperature scaling was estimated to be  $\sim 3.0 \times 10^{-6}$  and  $\sim 2.2 \times 10^{-6} \text{ m}^3/\text{mol}$  for  $\text{MgSiO}_3$  perovskite and  $\text{MgO}$ , respectively.

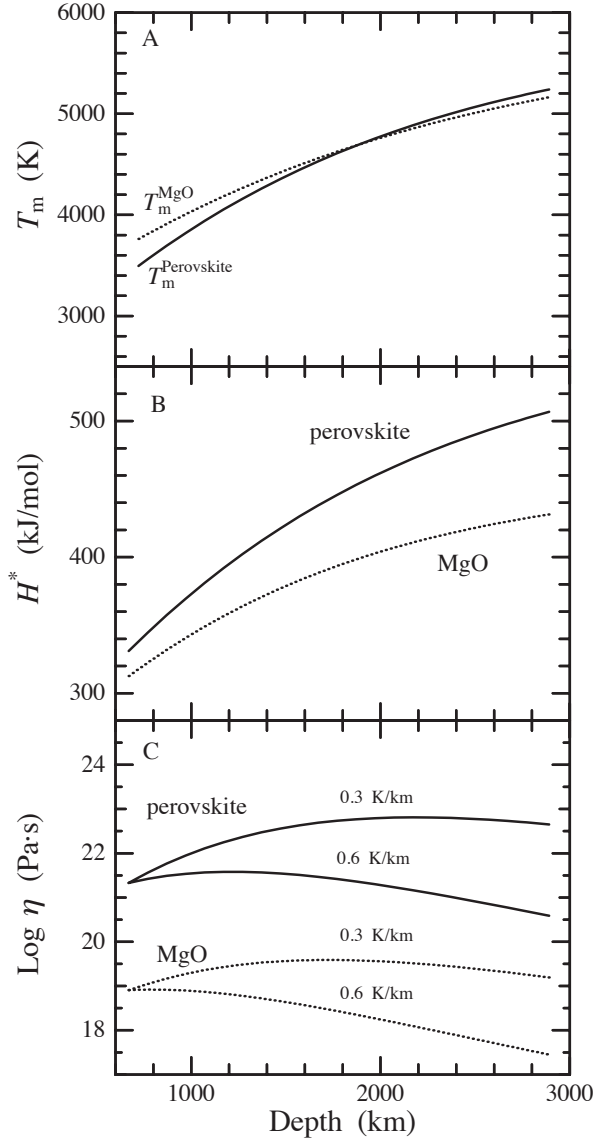


**FIGURE 2.** The results of the homologous temperature scaling model. (A) Solid line = melting temperatures of  $\text{MgSiO}_3$  perovskite with depth from Wang (1999) and dotted line = that of  $\text{MgO}$  from Zerr and Bohler (1994). (B) Estimated activation enthalpies for diffusion with depth for  $\text{MgSiO}_3$  perovskite and  $\text{MgO}$ . (C) Viscosity-depth profiles of  $\text{MgSiO}_3$  perovskite and  $\text{MgO}$  corresponding to the activation enthalpies shown in Figure 2B for the temperature gradients of 0.3 and 0.6 K/km. Grain size is assumed to be 3 mm.

Using Equation 1, viscosity variations in the lower mantle were calculated for  $\text{MgSiO}_3$  perovskite and  $\text{MgO}$ , assuming the grain size in the lower mantle is 3 mm, independent of depth, which corresponds to a viscosity at 25 GPa of  $10^{21}$ – $10^{22}$  Pa·s for perovskite (Fig. 2C) (The viscosities inferred from geodynamical observations are  $10^{20}$ – $10^{22}$  Pa·s; e.g., Peltier 1996). The grain size of 3 mm is similar to that of upper mantle

rocks (~1–10 mm; Avé Lallemant et al. 1980). Two temperature gradients, 0.3 and 0.6 K/km, were used to calculate the viscosity profile. The temperature gradient of ~0.3 K/km corresponds closely to the adiabatic gradient and ~0.6 K/km to a superadiabatic gradient. Both MgSiO<sub>3</sub> perovskite and MgO show slightly increasing viscosity with depth for 0.3 K/km gradients, on the other hand, they show slightly decreasing viscosity with depth for 0.6 K/km gradients (Fig. 2C).

### Elastic strain energy model

An alternative to the homologous temperature scaling is an elastic strain model. Assuming that the activation energy for diffusion is related to the strain energy of a crystal, Keyes derived an equation for activation enthalpy, viz., (Keyes 1963),

$$H^*(P) = \beta C(P) \Omega(P) \quad (8)$$

where  $\beta$  is a non-dimensional constant,  $C(P)$  is a combination of elastic constants and  $\Omega(P)$  is the molar volume. This relation gives results similar to homologous temperature scaling (Eq. 5) when melting behavior is related to lattice vibrations through Lindemann's model (Poirier and Liebermann 1984). The activation volume is estimated using the following equation

$$V^* = \frac{2H^*}{K} \left( \gamma - \frac{1}{3} \right) \quad (9)$$

where  $\gamma$  is Grüneisen parameter and  $K$  is the bulk modulus. A detailed discussion of the physical basis of this relation was given in Sammis et al. (1981) and Karato (1981b). Within the framework of the elastic strain energy model,  $C(P)$  is some combination of shear modulus and bulk modulus. The parameters used are summarized in Table 1.

The activation volume at 25 GPa was estimated to be  $\sim 3.0 \times 10^{-6}$  and  $2.2 \times 10^{-6}$  m<sup>3</sup>/mol for MgSiO<sub>3</sub> perovskite and MgO, respectively (Figs. 3A and 3B). Because MgSiO<sub>3</sub> perovskite

has a larger incompressibility than MgO, at depths greater than ~1400 km the activation enthalpy of MgO becomes larger than that of MgSiO<sub>3</sub> perovskite (Fig. 3B).

Similar to the case of the homologous temperature scaling, we calculated the viscosity-depth profiles, assuming a constant grain size of 3 mm and temperature gradients of 0.3 and 0.6 K/km (Fig. 3C). In the deepest portions in the lower mantle, the difference in viscosity between MgSiO<sub>3</sub> perovskite and MgO becomes small because of the larger activation volume of MgO than MgSiO<sub>3</sub> perovskite.

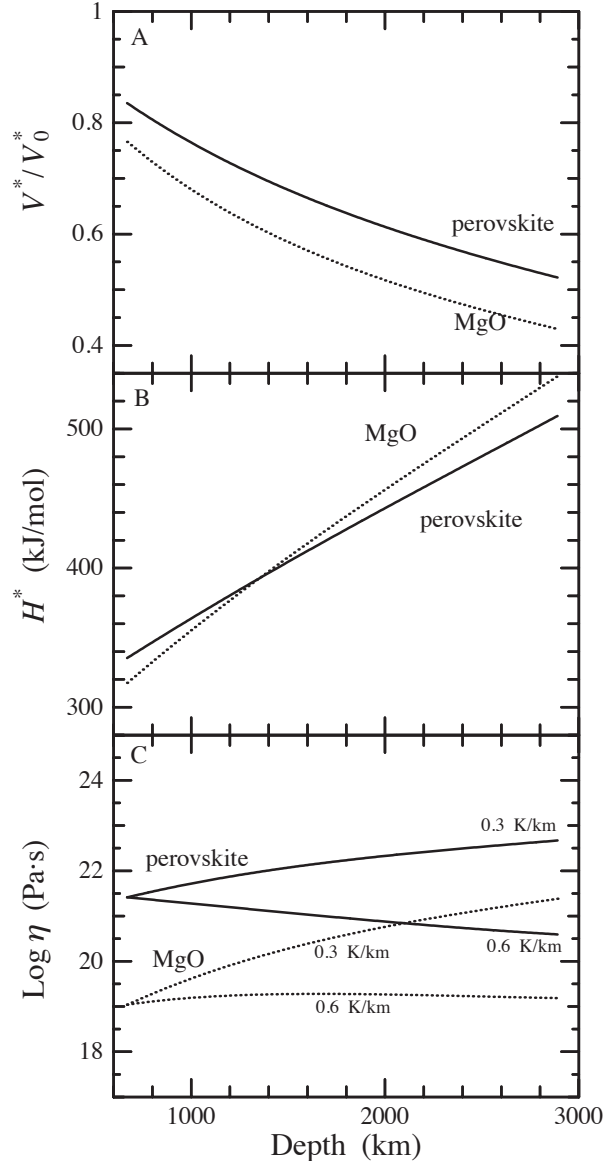


**FIGURE 3.** The results of the elastic strain energy model. (A) The change of the activation volume with depth for MgSiO<sub>3</sub> perovskite and MgO normalized by  $V_0$ , the activation volume at 0 GPa. (B) The activation enthalpy with depth corresponding to the activation volume shown in Figure 3A. (C) Viscosity-depth profiles for the temperature gradients of 0.3 and 0.6 K/km. Grain size is assumed to be 3 mm.

**TABLE 1.** Parameters used in the calculation of viscosities for MgSiO<sub>3</sub> perovskite and MgO

	MgSiO <sub>3</sub> perovskite	MgO
Pre-exponential factor	$D_0 = 2.7 \times 10^{-10} \text{ m}^2/\text{s}^*$ , $\delta D_0 = 7.1 \times 10^{-17} \text{ m}^3/\text{s}^\dagger, \S$	$6.1 \times 10^{-8} \text{ m}^2/\text{s}^\ddagger$
Activation enthalpy, $H^*$	336 kJ/mol <sup>†,*</sup> , 311 kJ/mol <sup>†,§</sup>	244 kJ/mol (1 atm) <sup>‡</sup>
Bulk modulus, $K_T$	261 GPa <sup>  </sup>	160 GPa <sup>#</sup>
$dK/dP$	4 <sup>  </sup>	4 <sup>#</sup>
Grüneisen parameter, $g$	1.4 <sup>**</sup>	1.5 <sup>#</sup>
Homologous temperature scaling factor, $g$	14 <sup>††</sup>	10 <sup>††</sup>

Notes: We use isothermal Bulk modulus,  $K_T$ . The difference between isothermal ( $K_T$ ) and adiabatic bulk modulus ( $K_S$ ) does not result in significant difference in our calculations.

\* For lattice diffusion at 25 GPa.

† Yamazaki et al. 2000.

‡ Passmore et al. 1966.

§ For grain boundary diffusion at 25 GPa.

|| Wang et al. 1994.

# Anderson and Isaak 1995.

\*\* Anderson 1998.

†† See text.

### EFFECTS OF A TWO-PHASE MIXTURE

The Earth's lower mantle is considered to be composed of 0–30% (Mg,Fe)O and 70–100% (Mg,Fe)SiO<sub>3</sub> perovskite (e.g., Ringwood 1991). Our present calculations show that, although MgO periclase is volumetrically a minor component, it has a significantly lower viscosity than that of MgSiO<sub>3</sub> perovskite. Therefore the averaging scheme must be critically evaluated when estimating the viscosity of the lower mantle.

Handy (1994) developed flow laws for a mixture of two viscous phases. He showed that mylonitic rocks and rock-analog materials had two basic types of structure: (1) a load-bearing framework (LBF) of a strong phase containing isolated pockets of a weak phase; (2) an interconnected layer of a weak phase (IWL) separating boudins and clasts of a strong phase. Takeda (1998) proposed a two-phase flow law model on the basis of the continuum physics of a multiphase assemblage. He suggested two models: one is a linear relationship between bulk viscosity and the volume fraction of the constituent minerals (i.e., homologous strain), corresponding to a case where a weaker phase is isolated (LBF), and (2) a non-linear relationship (i.e., homologous stress) corresponding to a case where a weaker phase forms a connected film (IWL).

From the derived viscosities of MgSiO<sub>3</sub> perovskite and periclase (Figs. 2 and 3), we can calculate the viscosities of the lower mantle using an appropriate averaging scheme. For this, we need (1) the volume fraction of each phase and (2) the geometry of each phase. Because the mineralogical composition of the lower mantle is not precisely known, we used a range of mixing ratio, i.e., 0 to 30 vol% of periclase. Following Takeda (1998), we calculated viscosities of a lower mantle assemblage corresponding to two end-member situations (IWL and LBF types): IWL type structure gives the lower bound and LBF type gives the upper bound for the viscosity of a two-phase mixture (Fig. 4).

Experimental studies show that a statically annealed mixture of (Mg,Fe)SiO<sub>3</sub> perovskite and (Mg,Fe)O has microstructures similar to the LBF case (Ito and Sato 1991; Yamazaki et al. 1996) whereas geometries closer to the IWL case are observed after large shear strain deformation (Yamazaki et al. 1999). Similarly, the transition in mechanical behavior from LBF to IWL type with increasing strain was observed in large strain deformation experiments on anhydrite and halite mixture (Ross et al. 1987). We calculated the grain-size to be ~3 mm near the top of the lower mantle where the viscosity is best constrained from geodynamical studies (e.g., Mitrovica and Forte 1997) assuming the upper-bound relation. We assume that the grain-size is independent of depth. The difference in viscosity between the two cases is as much as a factor of ~10 to 1000 at 30% volume fraction of MgO (Fig. 4). If the IWL type structure occurs, a small amount of a weaker phase (~3% of volume fraction of MgO) is much more effective in reducing the bulk viscosity when the viscosity contrast between MgSiO<sub>3</sub> perovskite and MgO is large (Figs. 4A and 4B in the case of the homologous temperature scaling), although the effect is less pronounced when the viscosity contrast is small (Figs. 4C and 4D in the case of the elastic strain energy model).

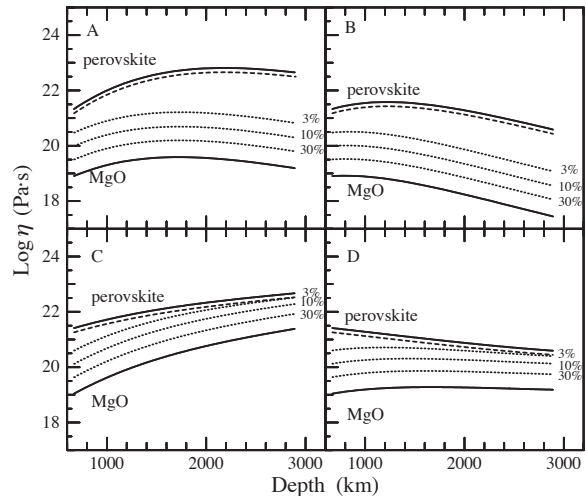


**FIGURE 4.** The viscosity-depth profiles in the lower mantle calculated by Takeda's (1998) model of deformation of a two phase mixture (MgSiO<sub>3</sub> perovskite and periclase) by. Solid lines represent the viscosity variation of MgSiO<sub>3</sub> perovskite and MgO, respectively, as shown in Figures 2C and 3C. Dotted lines represent the viscosity of a two phase mixture with an interconnected layer of a weak phase type structure (IWL) for various volume fractions of MgO, labeled in percent. Dashed lines show the viscosity of two phase mixture of a load-bearing framework type structure (LBF). In the later case, the viscosity is only weakly dependent on the volume fraction of MgO and the results for 30% MgO are shown. (A) Homologous temperature scaling;  $dT/dz = 0.3$  K/km, (B) Homologous temperature scaling;  $dT/dz = 0.6$  K/km, (C) Elastic strain energy model;  $dT/dz = 0.3$  K/km, (D) Elastic strain energy model;  $dT/dz = 0.6$  K/km.

### DISCUSSION

Using the latest results of laboratory measurements of diffusion coefficients of Si in perovskite (Yamazaki et al. 2000), diffusion creep in MgO (Passmore et al. 1966) and models of the pressure dependence of diffusion, we show that magnesiowüstite has significantly smaller viscosities than (Mg,Fe)SiO<sub>3</sub> perovskite, as previously suggested (e.g., Karato 1981a). This conclusion is insensitive to the details of models for pressure dependence of diffusion coefficients. However, several points may be worth some discussion in relation to the pressure dependence of diffusion coefficients, because significantly different on viscosity profiles can result from different models for effects of pressure.

From the homologous temperature scaling, we use the melting temperature of each phase rather than the solidus of the system. The solidus and the melting temperatures of constituent materials can be very different in some systems (e.g., Takahashi and Kushiro 1983 for peridotite; Zerr et al. 1998 for the lower mantle assembly), and this leads to large differences in estimated diffusion coefficients and hence viscosities. Karato (1998b) showed that the existing data on peridotites are inconsistent with scaling using the solidus temperature, because the addition of pyroxene to olivine significantly reduces the soli-



dus but has only a minor effect on deformation. The experimental results on the effects of pressure on deformation of olivine (Karato and Rubie 1997) are consistent with the homologous temperature scaling when the melting temperature of olivine is used. Therefore we consider that the use of the melting temperatures of constituent materials is more appropriate. Second, some limitations have been discussed on the elastic strain energy model for thermally activated processes. Karato (1981b) showed that such a model does not work well for ionic crystals where the contribution from electrostatic energy is significant. Despite these uncertainties, the inference of large rheological contrasts between the two phases [(Mg,Fe)SiO<sub>3</sub> perovskite and magnesiowüstite] seems robust.

This large contrast in viscosity of the two-phase assemblage means that the geometry of these two phases, as well as their volume fractions strongly influences on the viscosity of the lower mantle. Most of the well-annealed mixtures of MgO and MgSiO<sub>3</sub> perovskite (and their analogs) show LBF type microstructure where a weak MgO phase is isolated within the perovskite framework. In this case, the viscosity of the lower mantle is determined largely by that of (Mg,Fe)SiO<sub>3</sub> perovskite. In contrast, after large shear strains, a weak phase tends to form a continuous film and the viscosity of a two-phase mixture decreases significantly with strain. Handy (1994) and Takeda (1998) both suggested that deformed two-phase (or multi-phase) materials often show this IWL type microstructure and rheological data are more consistent with this model than LBF type model. We suggest that a strong LBF type structure may be appropriate in a stagnant core of a convection cell in the lower mantle, where the time scale for microstructural equilibrium is shorter than the time scale for shear, whereas in convecting boundary layers a weak IWL type structure may develop. In this case, the viscosity profile inferred from post-glacial rebound will correspond to that of LBF structure, whereas viscosities in the boundary layer will correspond to that of IWL. We suggest that the viscosity of the lower mantle is strain dependent due to the evolution of microstructure with strain.

We also notice that the depth variation in viscosity is modest for these models. The main reason for this is the small activation enthalpies for diffusion in MgSiO<sub>3</sub> perovskite and periclase. Small activation enthalpies for Si diffusion in perovskite (Yamazaki et al. 2000) and for creep in MgO (Passmore et al. 1966) are also consistent with the geodynamic inference of activation enthalpy by Cadek and van den Berg (1998). Therefore, a nearly depth-independent constant viscosity inferred from geodynamical modeling (e.g., Mitrova and Forte 1997) can be reconciled with a nearly adiabatic temperature gradient. However, this conclusion is highly dependent upon several poorly constrained mineral physics parameters such as the pressure dependence of melting temperatures. A significantly superadiabatic temperature gradient can also be consistent with viscosity profiles, if a stronger pressure dependence on melting temperatures is assumed (Zerr and Boehler 1993; Cohen and Weitz 1998).

Our analysis highlights the large difference in viscosity between MgSiO<sub>3</sub> perovskite and MgO and the importance of microstructural evolution in deforming two-phase aggregates. Although some models have been proposed to describe the rheo-

logical behavior of such rocks, no systematic experimental studies or theoretical works have been conducted on the flow of a two-phase aggregate. Further studies on the flow of a two-phase mixture is critical to better understand the rheology of the lower mantle and its influence on the evolution of Earth.

Very large uncertainties still exist as to the rheological behavior and other related properties of minerals at high pressures. For example, constraints are lacking on the effect of the substituting elements (e.g., Fe, Al, Ca) the slowest species for diffusion in MgSiO<sub>3</sub> perovskite and on the melting temperatures of MgSiO<sub>3</sub> perovskite and periclase. Our approach does not include effects of these other chemical species. Within a framework of homologous melting temperature scaling, the effects of these species could be incorporated through their effects on melting temperatures. Wang (1999) calculated that the effect of Al and Ca on the melting temperature of perovskite should be modest. Therefore we consider that the effects of these chemical species on rheology will not be very large. Obviously improved experimental studies on these effects under extreme conditions are needed in this area.

Finally, we note that the assumption of diffusion creep applies only to the bulk of the lower mantle away from the boundary layers. In the boundary layers such as the D'' layer evidence for seismic anisotropy is strong (e.g., Lay et al. 1998) suggesting the dominant role of dislocation creep (Karato 1998a).

## ACKNOWLEDGMENTS

We thank J.H. Jones, W.S. Kiefer, and Dave Walker for their comments. D. Yamazaki has been supported by Research Fellowships of the JSPS for Young Scientists. This work is partly supported by a grant from NSF (EAR-9805217).

## REFERENCES CITED

- Anderson, O.L. (1998) Thermoelastic properties of MgSiO<sub>3</sub> perovskite using the Debye approach. *American Mineralogist*, 83, 23–35.
- Anderson, O.L. and Isaak, D.G. (1995) Elastic constants of mantle minerals at high temperature. In T.J. Ahrens, Ed., *Mineral Physics and Crystallography, A Handbook of Physical Constants*, pp. 64–97. American Geophysical Union, Washington, D.C.
- Avé Lallemant, H.G., Mercier, J.-C.C., Carter, N.L., and Ross, J.V. (1980) Rheology of the upper mantle: inferences from peridotite xenoliths. *Tectonophysics*, 70, 85–113.
- Cadek, O. and van den Berg, A.P. (1998) Radial profile of temperature and viscosity in the Earth's mantle inferred from the geoid and lateral seismic structure. *Earth and Planetary Science Letters*, 164, 607–615.
- Cohen, R.E. and Weitz, J.S. (1998) The melting curve and premelting of MgO. In M.H. Manghnani and T. Yagi, Eds., *Properties of Earth and Planetary Materials at High Pressure and Temperature*, Geophysics Monograph Series vol. 101, p. 185–196. AGU, Washington, D.C.
- Frost, H.J. and Ashby, M.F. (1982) *Deformation mechanism maps*, 168 p. Pergamon Press, Oxford, U.K.
- Garnero, E.D. and Lay, T. (1997) Lateral variations in lowermost mantle shear wave anisotropy beneath the north Pacific and Alaska. *Journal of Geophysical Research*, 102, 8121–8135.
- Gordon, R.S. (1985) Diffusional creep phenomena in polycrystalline oxides. In R.N. Schock, Ed., *Point Defects in Minerals*, Geophysics Monograph Series vol. 31, p. 132–140. AGU, Washington, D.C.
- Handy, M.R. (1994) Flow laws for rocks containing two non-linear viscous phases: a phenomenological approach. *Journal of Structural Geology*, 16, 287–301.
- Ito, E. and Katsura, T. (1989) A temperature profile of the mantle transition zone. *Geophysical Research Letters*, 16, 425–428.
- Ito, E. and Sato, H. (1991) Aseismicity in the lower mantle by superplasticity of the descending slab. *Nature*, 351, 140–141.
- Jaoul, O., Poumellec, M., Froidevaux, C., and Havette, A. (1981) Silicon diffusion in forsterite: a new constraint for understanding mantle deformation. In F.D. Stacey et al., Eds., *Anelasticity in the Earth*, Geodynamical Series vol. 4, p. 95–100. American Geophysical Union, Washington, D.C.
- Jaoul, O., Houlier, B., and Abel, F. (1983) Study of <sup>18</sup>O diffusion in magnesium orthosilicate by nuclear microanalysis. *Journal of Geophysical Research*, 88, 613–624.

- Karato, S. (1981a) Rheology of the lower mantle. *Physics of the Earth and Planetary Interiors*, 24, 1–14.
- (1981b) Pressure dependence of diffusion in ionic solids. *Physics of the Earth and Planetary Interiors*, 25, 38–51.
- (1988) The role of recrystallization in the preferred orientation of olivine. *Physics of the Earth and Planetary Interiors*, 51, 107–122.
- (1998a) Some remarks on the origin of seismic anisotropy in the D'' layer. *Earth, Planets and Space*, 50, 1019–1028.
- (1998b) Effects of pressure on plastic deformation of polycrystalline solids: Some geological applications. In R.M. Wentzcovitch et al., Eds., *High-Pressure Materials Research*, Materials Research Society Symposium Proceeding vol. 499, p. 3–14. Materials Research Society, Warrendale, Pennsylvania.
- Karato, S. and Li, P. (1992) Diffusion creep in perovskite: Implication for the rheology of the lower mantle. *Science*, 255, 1238–1240.
- Karato, S., Paterson, M.S., and FitzGerald, J.D. (1986) Rheology of synthetic olivine aggregates: Influence of grain size and water. *Journal of Geophysical Research*, 91, 8151–8176.
- Karato, S., Zhang, S., and Wenk, H.R. (1995) Superplasticity in Earth's lower mantle: Evidence from seismic anisotropy and rock physics. *Science*, 270, 458–461.
- Karato, S. and Rubie, D.C. (1997) Toward an experimental study of deep mantle rheology: A new multianvil sample assembly for deformation studies under high pressure and temperature. *Journal of Geophysical Research*, 102, 20111–20122.
- Keyes, R.W. (1963) Continuum models of the effect of pressure on activated processes. In W. Paul and D. Warshauer, Eds., *Solids under Pressure*, p. 71–91, McGraw Hill, N.Y.
- Lay, T., Williams, Q., and Garnero, E.D. (1998) The core-mantle boundary layer and deep Earth dynamics. *Nature*, 392, 461–468.
- Li, P., Karato, S., and Wang, Z. (1996) High-temperature creep in fine-grained polycrystalline  $\text{CaTiO}_3$ , an analogue material of  $(\text{Mg,Fe})\text{SiO}_3$  perovskite. *Physics of the Earth and Planetary Interiors*, 95, 19–36.
- Meade, C., Silver, P.G., and Kaneshima, S. (1995) Laboratory and seismological observations of lower mantle isotropy. *Geophysical Research Letters*, 22, 1293–1296.
- Mitrovica, J.X. and Forte, A.M. (1997) Radial profile of mantle viscosity: Results from the joint inversion of convection and postglacial rebound observables. *Journal of Geophysical Research*, 102, 2751–2769.
- Montagner, J.-P. and Kennett, B.L.N. (1996) How to reconcile body-wave and normal-mode reference Earth model. *Geophysical Journal International*, 125, 229–248.
- Passmore, E.M., Duff, R.H., and Vasilos, T. (1966) Creep of dense, polycrystalline magnesium oxide. *Journal of the American Ceramic Society*, 49, 594–600.
- Peltier, W.R. (1996) Mantle viscosity and ice-age ice sheet topography. *Science*, 1359–1364.
- Poirier, J.P., Peyronneau, J., Gesland, J.Y., and Brebec, G. (1983) Viscosity and conductivity of the lower mantle; an experimental study on a  $\text{MgSiO}_3$  perovskite analogue,  $\text{KZnF}_3$ . *Physics of the Earth and Planetary Interiors*, 32, 273–287.
- Poirier, J.P. and Liebermann, R.C. (1984) On the activation volume for creep and its variation with depth in the Earth's lower mantle. *Physics of the Earth and Planetary Interiors*, 35, 283–293.
- Ringwood, A.E. (1991) Phase transformations and their bearing on the constitution and dynamics of the mantle. *Geochimica et Cosmochimica Acta*, 55, 2083–2110.
- Ross, J.V., Bauer, S.J., and Hansen, F.D. (1987) Textural evolution of synthetic anhydrite-halite mylonites. *Tectonophysics*, 140, 307–326.
- Sammis, C.G., Smith, J.C., and Schubert, G. (1981) A critical assessment of estimation methods for activation volume. *Journal of Geophysical Research*, 86, 10707–10718.
- Sherby, O.D., Robbins, J.L., and Goldberg, A. (1970) Calculation of activation volumes for self-diffusion and creep at high temperature. *Journal of Applied Physics*, 41, 3961–3968.
- Stocker, R.L. and Ashby, M.F. (1973) On the rheology of the upper mantle. *Review of Geophysics and Space Physics*, 11, 391–426.
- Takahashi, E. and Kushiro, I. (1983) Melting of a dry peridotite at high pressure and basalt magma genesis. *American Mineralogist*, 68, 859–879.
- Takeda, Y. (1998) Flow in rocks modelled as multiphase continua: application to polymineralic rocks. *Journal of Structural Geology*, 20, 1569–1578.
- Wall, A. and Price, G.D. (1989) Defects and diffusion in  $\text{MgSiO}_3$  perovskite: A computer simulation. In A. Navrotsky and D.J. Weidner, Eds., *Perovskite: A Structure of Great Interest to Geophysics and Materials Science*, Geophysical Monograph Series vol. 45, p. 45–53. American Geophysical Union, Washington, D.C.
- Wang, Y., Weidner, D.J., Liebermann, R.C., and Zhao, Y. (1994) P-V-T equation of state of  $(\text{Mg,Fe})\text{SiO}_3$  perovskite: Constraints on composition of the lower mantle. *Physics of the Earth and Planetary Interiors*, 83, 13–40.
- Wang, Z.W. (1999) The melting of Al-bearing perovskite at the core-mantle boundary. *Physics of the Earth and Planetary Interiors*, 115, 219–228.
- Weertman, J. (1970) The creep strength of the Earth's mantle. *Review of Geophysics and Space Physics*, 8, 145–168.
- Yamazaki, D., Kato, T., Ohtani, E. and Toriumi, M. (1996) Grain growth rates of  $\text{MgSiO}_3$  perovskite and periclase under lower mantle conditions. *Science*, 274, 2052–2054.
- Yamazaki, D., Lee, K.-H. and Karato, S. (1999) Deformation experiments on  $\text{MnTiO}_3$  +  $\text{MnO}$  as an analogue of lower mantle minerals. *EOS transaction*, 80: F758. American Geophysical Union abstract.
- Yamazaki, D., Kato, T., Yurimoto, H., Ohtani, E., and Toriumi, M. (2000) Silicon self-diffusion in  $\text{MgSiO}_3$  perovskite at 25 GPa. *Physics of the Earth and Planetary Interiors*, 119, 299–309.
- Zerr, A. and Boehler, R. (1993) Melting of  $(\text{Mg,Fe})\text{SiO}_3$ -perovskite to 625 kilobars: Indication of a high melting temperature in the lower mantle. *Science*, 262, 553–555.
- (1994) Constraints on the melting temperature of the lower mantle from high-pressure experiments on  $\text{MgO}$  and magnesio-wüstite. *Nature*, 371, 506–508.
- Zerr, A., Diegeler, A. and Boehler, R. (1998) Solidus of earth's deep mantle. *Science*, 281, 243–246.

MANUSCRIPT RECEIVED APRIL 18, 2000  
 MANUSCRIPT ACCEPTED DECEMBER 20, 2000  
 MANUSCRIPT HANDLED BY JOHN H. JONES